Algorithm Technical Background Document

NASA VIIRS Burned Area Product

Version 1.1
July 2017

Louis Giglio, Luigi Boschetti, David Roy, and Christopher Justice

(NASA VIIRS Science Team)

1. Introduction

1.1 Science/Applications Rationale

As Earth System Science studies increasingly recognize and include fire as an important process in the terrestrial carbon cycle, there is a growing need for long term, spatially- and temporally-explicit global burned area data sets. The advent of NASA's Terra and Aqua satellites has enabled, for the first time, systematic production of high quality, multi-year, 500-m global burned area maps using observations from the Moderate Resolution Imaging Spectroradiometer (MODIS). The MODIS fire datasets have been used in the scientific literature more than any other global fire dataset (Mouillot et al., 2013). Both the global modeling community and the fire applications community are using these data (e.g., Korontzi et al., 2004; Jin and Roy, 2005; Archibald et al., 2009; van der Werf et al., 2010; Granier et al. 2011; Giglio et al. 2013). There is considerable interannual variability in the distribution and extent of fires (Kasischke and Turetsky, 2006; Westerling et al., 2006; Pausas et al., 2012; Chen et al., 2013) but long-term, consistent observation records are necessary for analyzing the relationship between climate and fire regimes.

A critical step in the establishment of a long-term global burned area record is ensuring the transition from the aging MODIS instrument data to the Visible Infrared Imaging Radiometer Suite (VIIRS) data provided by the current Suomi National Polar-orbiting Partnership (NPP) and the forthcoming Joint Polar Satellite System (JPSS). NPP serves as a risk reduction for the JPSS and has a programmatic emphasis on short-term operational weather forecasting and military applications (Murphy et al., 2006). Consequently only a VIIRS active fire product was mandated in the NPOESS Integrated Operational Requirements Document (IORD) and in the successor JPSS Level 1 Requirements Document. No burned area product was mandated. This is despite the fundamental issue that the area burned cannot be estimated reliably from satellite active fire detections because (i) the satellite may not overpass when burning occurs, (ii) clouds and optically thick smoke may preclude active fire detection, and, (iii) small and cool fires may not be detected (Giglio, 2007; Roy et al., 2008). The forthcoming VIIRS "SNP64A1" burned area product remedies this omission.

1.2 Intended User Community

The VIIRS SNP64A1 burned area product is an interdisciplinary data set designed to meet the needs of the global change research and the fire applications community. The product is intended as a replacement for the existing and widely used MODIS MCD64A1 burned area product.

2. Burned Area Mapping Algorithm

2.1 Technical Background and Heritage

A major objective in producing the NASA VIIRS burned area data record is to continue the 18-year MODIS burned area time series into the Suomi-NPP and JPSS era, and form the basis for a climate data record. The mapping approach is consequently based on the existing MODIS Collection 6 MCD64 burned-area mapping algorithm developed by our team for the MODIS instrument (Giglio et al., 2009). The algorithm maps the spatial extent of recent fires and not of

fires that occurred in previous seasons or years. The VIIRS burned area product is identified as SNP64A1.

2.2 Algorithm Description

The SNP64 burned-area mapping approach employs 750-m VIIRS imagery coupled with 750-m VIIRS active fire observations. The hybrid algorithm applies dynamic thresholds to composite imagery generated from a burn-sensitive vegetation index (VI) derived from VIIRS short-wave infrared channels M8 and M11, and a measure of temporal texture. The VI is defined as

$$VI = (\varrho_8 - \varrho_{11}) / (\varrho_8 + \varrho_{11}),$$

where ϱ_8 and ϱ_{11} are respectively the band M8 and band M11 atmospherically corrected surface reflectance. Cumulative active fire maps are used to guide the selection of burned and unburned training samples and to guide the specification of prior probabilities. The combined use of active-fire and reflectance data enables the algorithm to adapt regionally over a wide range of pre- and post-burn conditions and across multiple ecosystems. A detailed description of the algorithm can be found in Giglio et al. (2009).

The mapping algorithm ultimately identifies the date of burn, to the nearest day, for 500-m grid cells within the individual sinusoidal tile being processed. The date is encoded in a single data layer of the output product as the ordinal day of the calendar year on which the burned (range 1-366), with a value of 0 for unburned land pixels and additional special values reserved for missing-data and water grid cells. The output product contains additional data layers for diagnostic purposes and to facilitate uncertainty propagation into downstream products derived from the burned area maps, such as emissions estimates.

2.3 Product Description

For compatability with the existing MODIS MCD64A1 burned area product, three different versions of the SNP64A1 product will be available:

- The official SNP64A1 product in HDF5-EOS format, which will be available as part of the NASA VIIRS suite of global land products.
- The re-projected monthly GeoTIFF version, to be available from the University of Maryland.
- The re-projected monthly Shapefile version, to be available from the University of Maryland.

A complete description of each product will be provided in the forthcoming *SNP64A1 User's Guide*.

2.4 Product Prototype

As of this writing, the required 500-m gridded upstream VIIRS input products (Section 3) are not yet generated within NASA's Land SIPS, hence in the interim we have used lower resolution, gridded VIIRS data sets formerly produced by the Land SIPS for diagnostic purposes as proxy inputs. Specifically, we used the 1-km NPP_DSRFIP_L3 VIIRS diagnostic surface reflectance product as an interim source of daily VIIRS surface reflectance data, and the 1-km NPP_DAF1KM_L3D VIIRS diagnostic 8-day active fire product as a source of VIIRS active

fire data. As shown in Figure 1, the resulting burned area maps are in good agreement despite the degraded spatial resolution of the interim VIIRS products.

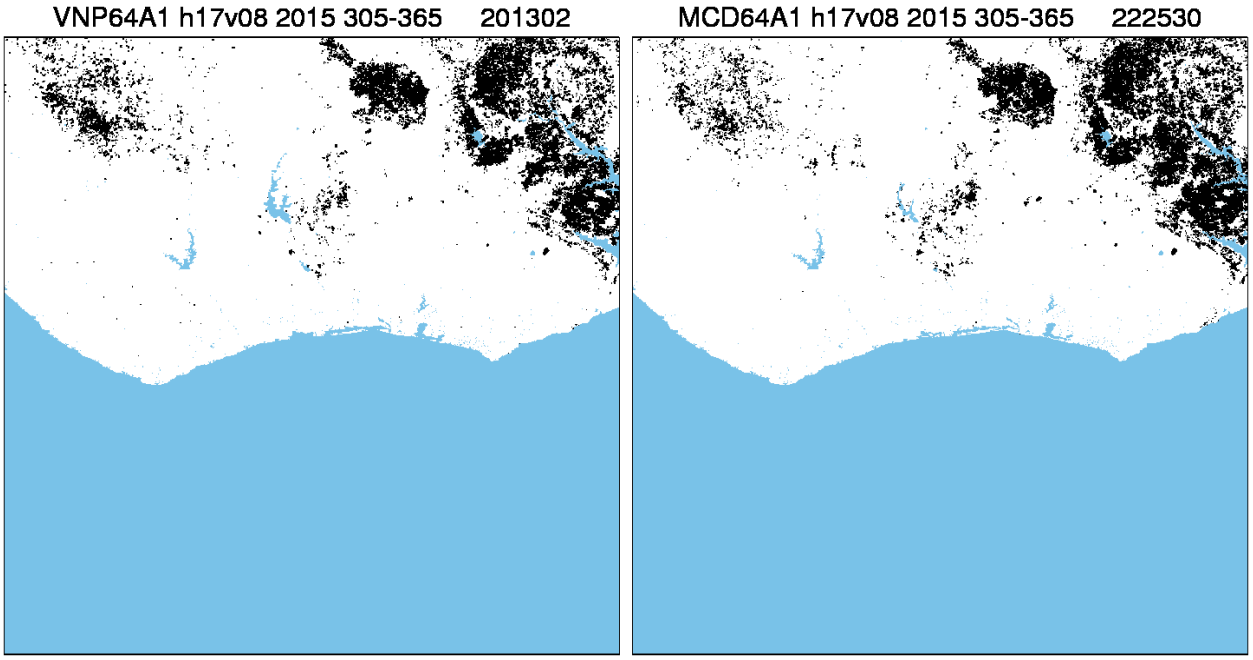

Figure 1: Example 1-km interim prototype VIIRS (left) and 500-m Collection 6 MODIS (right) cumulative burned area maps for 1 November – 31 December 2015 generated using the MCD64 burned area mapping algorithm applied to observations acquired from the respective sensors. This 1200 km × 1200 km tile is located in western Africa. Burned grid cells are shown in black, while white areas represent unburned portions of the landscape. Water is shown in blue.

3. Product Inputs

The VIIRS VNP64A1 burned area product will be generated from time series of daily 750-m VIIRS land surface reflectance data, resampled to the 500-m MODIS sinusoidal grid, and 750-m VIIRS active fire data, resampled onto the 1-km MODIS sinusoidal grid. A simplified overview of the VIIRS burned area processing chain is shown in Figure 2. As of this writing most of the required upstream inputs are not yet produced operationally within the Land SIPS.

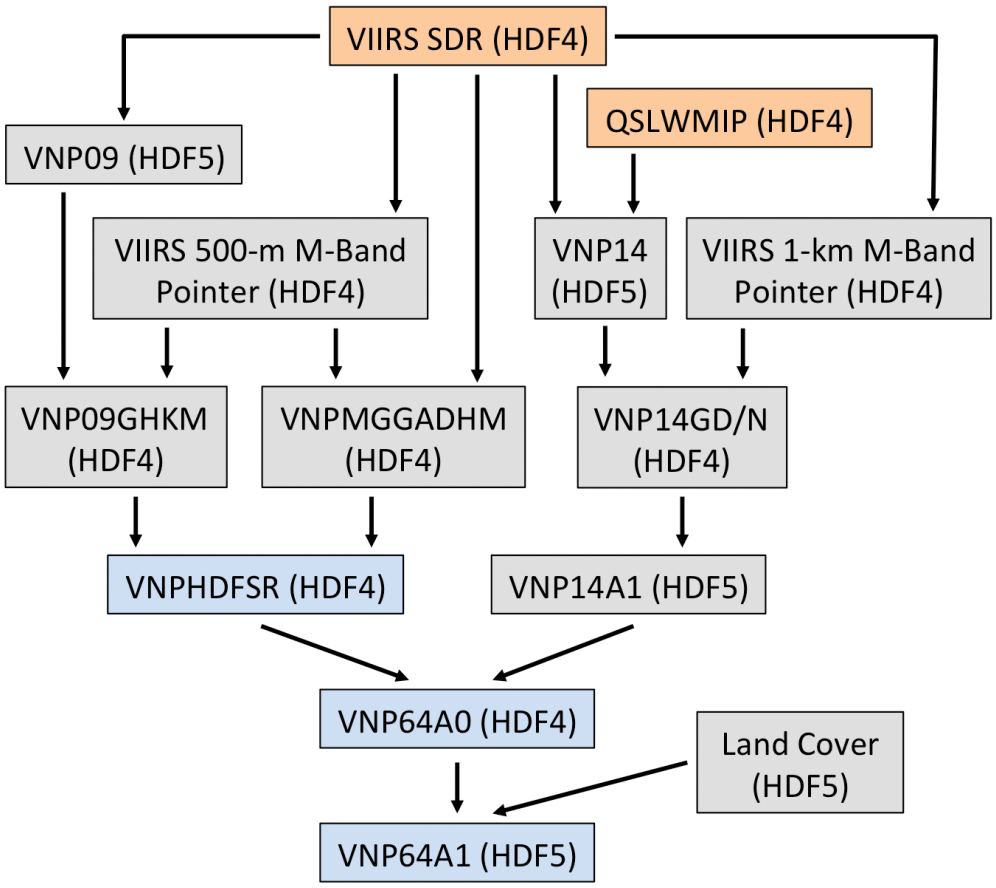

Figure 2: Flow diagram showing the planned input data stream for the VIIRS VNP64A0 (burned area intermediate) and VNP64A1 (monthly burned area) products. Each box represents a separate production code and VIIRS product, and indicates its current file format (either HDF4 or HDF5). The orange boxes highlight the interim VIIRS SDR (radiance/geolocation) and QSLWMIP (land/water mask) inputs in use until the improved NASA Level 1B radiance and geolocation products are adopted for VIIRS Land production. The prefixes "VNP09" and "VNP14" denote surface reflectance and active fire products, respectively. At present only the first three products in the processing chain (VIIRS SDR, QSLWMIP, and VNP09) are being generated within the Land SIPS.

3.1 Spectral Bands

VIIRS bands that are both sensitive and insensitive to biomass burning are used to detect changes due to fire and to differentiate them from other types of change. As established earlier with the MODIS instrument, near-infrared and longer wavelength reflective bands are used because they are generally insensitive to smoke aerosols emitted from vegetation fires (Kaufman and Remer 1994; Miura et al., 1998). An analysis of the ability of the MODIS land surface reflectance bands to discriminate between recently burned and unburned vegetation (Roy et al., 2002; Roy et al., 2005b) has shown that MODIS bands 5 [1230-1250 nm] and 2 [841-876 nm] provide the highest burned-unburned discrimination and MODIS band 7 [2105-2155 nm] provides little discrimination. Bands 5, 2 and 6 [1628-1652 nm] reflectance decreases immediately, and for many days, after burning, and band 7 reflectance changes relatively less (with both positive or negative changes observed).

Some surface changes not associated with biomass burning may exhibit similar spectral changes as those caused by fire. Depending on the algorithm and wavelengths used, this may cause false detections.

Examination of Figure 3 indicates that decreases in near-infrared and short wave infrared reflectance (MODIS bands 2 and 5) similar to those caused by burning may also occur with snow melt, vegetation removal exposing less reflective soil (e.g., due to harvesting or pests), flooding, and vegetation senes-cence. The Australian herbaceous plant spectra (green) show a typical reduction in the near-infrared (bands 2 and 5) and increase in red (band 1) reflectance as the vegetation senesces from lush green vegetation to dried material with 100% cover. The Zambian grass spectra (orange) show an opposite change and are included to illustrate the complexity of potential sources of spectral confusion. In the Zambia case, senescence from green, waterlogged grass (dashed orange) to dry grass on an exposed bright soil background (solid orange) increases the near-infrared and the other MODIS band reflectance. The Zambian example illustrates that increasing plant water content may reduce MODIS band 5, 6 and 7 reflectance but have less impact on band 2 reflectance (Zarco-Tejada et al., 2003). Shadows, cast by clouds and surface relief, are not illustrated, but generally reduce reflectance in all reflective bands and so exhibit similar spectral changes as those caused by fire (Roy et al., 2002).

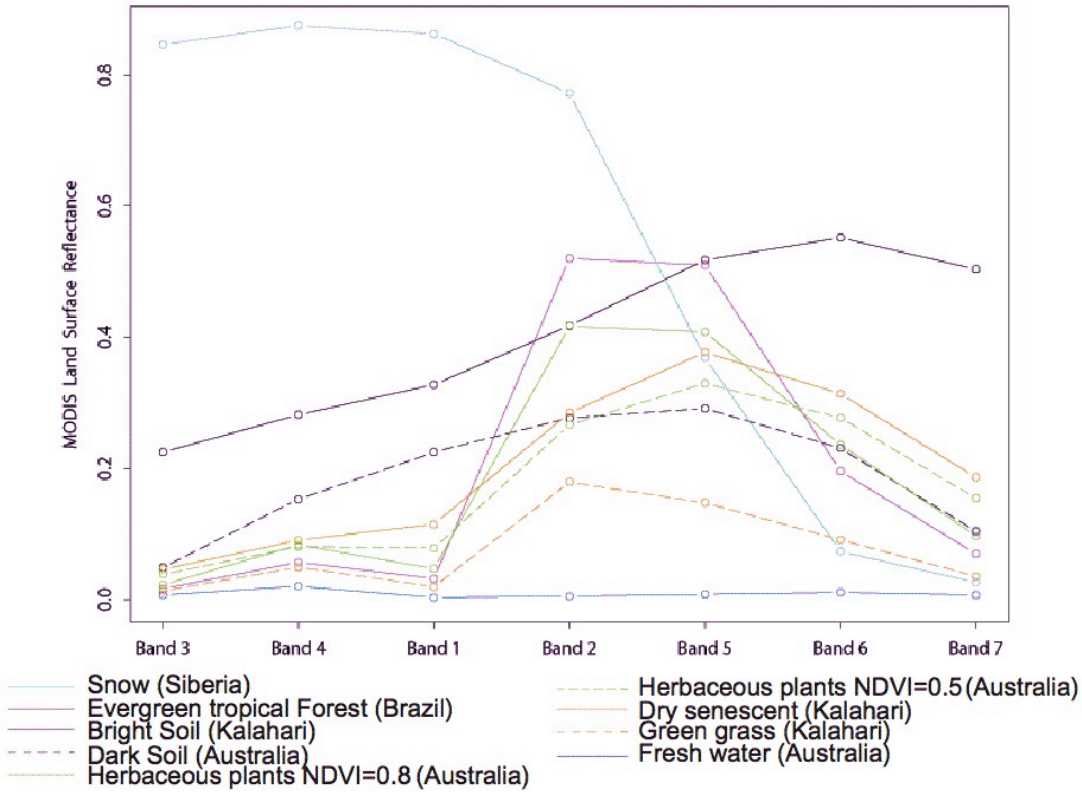

Figure 3: Illustrative MODIS reflective band spectra, derived from the mean reflectance of 25 cloud-free, near-nadir 500 m MODIS pixels for a number of different surface types.

The previously developed MODIS MCD64 and MCD45 burned area mapping algorithms exploit nearly the same 500-m MODIS bands; these are shown in Table 1 along with the equivalent 750-m "M-band" VIIRS channels. VIIRS also has five higher resolution (375-m) "I-band" channels, but these unfortunately cannot serve as seamless replacements for the 500-m MODIS bands used by the mapping algorithms as VIIRS lacks the necessary 1.2 μm and 2.1 μm bands at I-band resolution. For this reason, and for consistency with the 500-m MODIS burned area products, a "500-m" VIIRS burned area product will be generated from resampled 750-m VIIRS imagery.

Table 1. Bands used to generate the MODIS MCD45 (Collection 5.1) and MCD64 (Collection 6) burned area products with the corresponding 750-m and 375-m VIIRS bands.

MODIS Band	MODIS Central Wavelength (μm)	VIIRS 750-m Band	VIIRS Central Wavelength (μm)	Corresponding VIIRS 375-m Band
1	0.65	M5	0.67	I1
2	0.86	M7	0.87	I2
5	1.2	M8	1.2	-
7	2.1	M11	2.3	-
20	3.8	M12	3.7	I4

4. Product Accuracy/Uncertainty

4.1 Validation Approach

Accuracy assessment (validation) of the MODIS burned area products was developed in parallel with the development of the MODIS burned area mapping algorithms, providing a means to improve the product performance; starting from the early stage of testing on limited areas, the accuracy of the product was evaluated (CEOS Stage 1) using time series of high resolution Landsat 7 ETM+ data. This preliminary research led to the development of a validation protocol, specifically aimed at the production of accurate reference data for burned area maps, derived from high resolution data, for the validation of the burned area product. The protocol was developed initially in the context of the SAFARI 2000, southern Africa regional science initiative (Swap et al., 2002) by members of the GOFC/GOLD Southern African Fire Network (SAFNet) (Roy et al., 2005a). The SAFNet protocol after peer review became the basis for the International Burned Area Validation Protocol adopted by the CEOS Land Product Validation Working Group for use by the international community (Boschetti et al, 2010).

Given the impermanent nature of many burned areas, with a spectral signal that can disappear in as little as few weeks in certain savanna systems (Trigg and Flasse, 2000), and conversely the persistence of the burned signal for several years in boreal systems (Sukhinin et al., 2004), it is crucial to ensure that the time period covered by the high resolution reference data is clearly defined and the same as the satellite burned area time period being validated. The validation protocol therefore requires the use of multi-temporal pairs of Landsat-class imagery, allowing for comparison of the burned areas detected by the MODIS algorithm in the period between acquisitions.

4.2 Sampling Strategy

An extensive validation data set of Landsat-8 OLI image pairs has been selected, implementing the stratified random sampling strategy described in Boschetti et al. (2016), that allows for probability sampling of Landsat data in time and in space. To sample the globe in the spatial domain with non-overlapping sampling units, the Thiessen Scene Area (TSA) tessellation of the WRS path/rows is used. The TSA grid is then combined with the 16-day Landsat acquisition calendar to generate a tri-dimensional grid, where each element (voxel) corresponds to a Landsat image pair. The tri-dimensional grid is stratified through a two-level procedure. A first spatial stratification is based on seven global biomes, and ensures that the sample is well distributed across continents and vegetation types. The second level of stratification is temporal, and is conducted independently within the first level strata. It partitions the population of voxels into high and low fire activity strata, using as a stratification variable the number of MODIS active fires detected within the spatial and temporal extent of each voxel (Figure 4).

This stratification ensures that the randomly selected image pairs capture the spatial and temporal variability of global fire activity. The validation data set includes 700 randomly selected Landsat image pairs, equally allocated between the high and low fire activity strata of the 7 biomes (Figure 5).

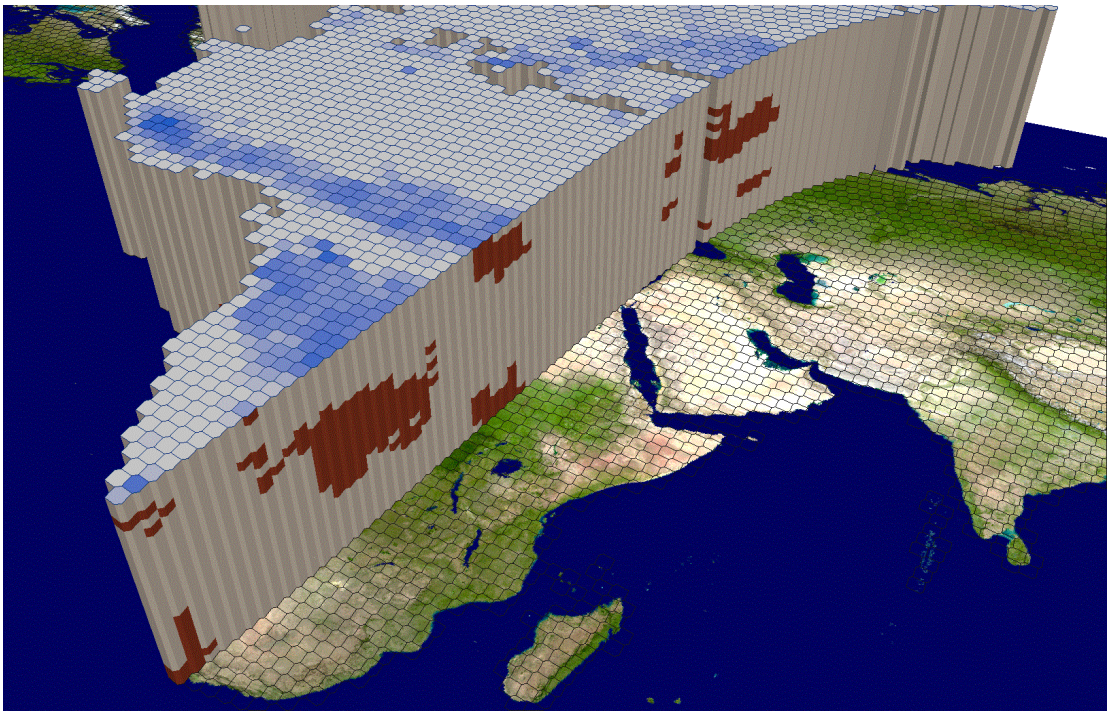

Figure 4: Tri-dimensional representation of the stratification of one year of Landsat 8 data for the purpose of extracting a sample of reference data. Red cells represent high fire activity; gray cells represent low fire activity. The cross section is cut along WRS path 175, and highlights the seasonality of fire in Africa: a fire season concentrated in the central months of the year south of the Equator, and at the both ends of the year north of the Equator. Shown on the top layer, in blue, is the conventional representation of the annual summary of fire activity at each WRS location.

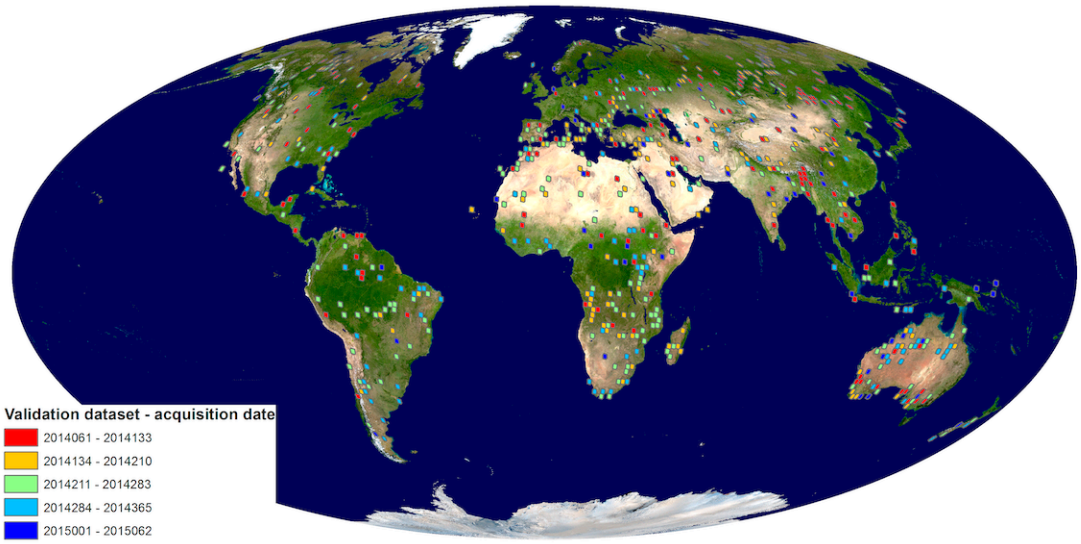

Figure 5: Spatial and temporal location of reference data set generated for validation of the MODIS and VIIRS burned area products. A total of 700 Landsat-8 OLI image pairs (100 in each biome) were selected.

4.3 Uncertainty Estimate

Uncertainty estimates will be produced following validation of the forthcoming SNP64A1 product.

5. Data Format

5.1 Format

Like its MODIS predecessor, the SNP64A1 product will contain five data layers (*Burn Date*, *Burn Date Uncertainty*, *QA*, *First Day*, and *Last Day*), each stored as a separate HDF5 Scientific Data Set (SDS).

Burn Date: Ordinal day of burn (1-366) for each 500-m grid cell, with 0 = unburned land, -1 = unmapped due to insufficient data, and -2 = water.

Burn Date Uncertainty: Estimated uncertainty in date of burn, in days. Unburned and unmapped grid cells will always have a value of 0 in this layer.

QA: 8-bit quality assurance bit field.

bit 0: 0 = water grid cell, 1 = land grid cell.

bit 1: Valid data flag (0 = false, 1 = true). A value of 1 indicates that there was sufficient valid data in the reflectance time series for the grid cell to be processed. (NB. Water grid cells will always have this bit clear.)

bit 2: Shortened mapping period (0 = false, 1 = true). This flag indicates that the period of reliable mapping does not encompass the full one-month product period, i.e., burns could not be reliably mapped over the full calendar month.

bit 3: Grid cell was relabeled during the contextual relabeling phase of the algorithm (0 = false, 1 = true).

bit 4: Spare bit set to 0.

bits 5–7: Special condition code reserved for unburned grid cells. This code provides an explanation for any grid cells that were summarily classified as unburned by the detection algorithm due to special circumstances.

0: None or not applicable (i.e., burned, unmapped, or water grid cell).

1: Valid observations spaced too sparsely in time.

2: Too few training observations or insufficient spectral separability between burned and unburned classes.

3: Apparent burn date at limits of time series.

4: Apparent water contamination.

5: Persistent hot spot.

6: Reserved for future use.

7: Reserved for future use.

First Day and *Last Day*: These layers indicate the first and last days, respectively, on which changes could be reliably detected within the time series, on a per-grid-cell basis. Note that during periods of persistent cloud cover or frequent data loss, these dates will often

lie within the calendar month that was mapped, indicating that reliable mapping could not be achieved over the full month.

5.2 QA Metadata

A complete description of all product quality assurance metadata will be provided following operational production of the SNP64A1 product within NASA's Land SIPS.

6. References

Archibald, S., Roy, D. P., Van Wilgen, B. W., and Scholes, R. J., 2009, What Limits Fire? An examination of drivers of burnt area in sub-equatorial Africa. *Global Change Biology*, 15, 613 - 630.

Boschetti, L., Roy, D. P. and Justice, C.O., 2010, CEOS International Global Burned Area Satellite Product Validation Protocol, Part I – production and standardization of validation reference data, available online http://lpvs.gsfc.nasa.gov/.

Boschetti, L., Stehman, S. V., and Roy, D. P., 2016, A stratified random sampling design in space and time for regional to global scale burned area product validation. *Remote Sensing of Environment*, 186, 465-478.

Chen, Y., Morton, D. C., Jin, Y., Gollatz, G. J., Kasibhatla, P. S., van der Werf, G. R., and Randerson, J. T., 2013, Long-term trends and interannual variability of forest, savanna and agricultural fires in South America. *Carbon Management*, 4(6), 617-638.

Giglio, L., Randerson, J. T., and van der Werf, G. R., 2013, Analysis of daily, monthly, and annual burned area using the fourth generation Global Fire Emissions Database (GFED4). *Journal of Geophysical Research: Biogeosciences*, 118.

Giglio, L., 2007, Characterization of the tropical diurnal fire cycle using VIRS and MODIS observations. Remote Sensing of Environment, 108, 407-421.

Giglio, L., Loboda, T., Roy, D. P., Quayle, B., and Justice, C. O., 2009, An active-fire based burned area mapping algorithm for the MODIS sensor. *Remote Sensing of Environment*, 36, 408-420.

Granier, C., Bessagnet, B., Bond, T., D'Angiola, A., Van Der Gon, H.D., Frost, G.J., Heil, A., Kaiser, J.W., Kinne, S., Klimont, Z., 2011, Evolution of anthropogenic and biomass burning emissions of air pollutants at global and regional scales during the 1980–2010 period, Climatic Change, 109: 163-190.

Jin, Y. and Roy, D. P., 2005, Fire-induced albedo change and its radiative forcing at the surface in northern Australia. *Geophysical Research Letters*, 32, L13401.

Kasischke, E. S., and Turetsky, M. R., 2006, Recent changes in the fire regime across the North American boreal region - Spatial and temporal patterns of burning across Canada and Alaska. *Geophysical Research Letters*, 33, L09703.

Kaufman, Y. J. and Remer, L., 1994, Detection of forests using mid-IR reflectance: An application for aerosol studies. *IEEE Transactions on Geoscience and Remote Sensing*, 32, 672-683.

Korontzi, S., Roy, D. P., Justice C. O., Ward, D. E., 2004, Modeling and sensitivity analysis of fire emissions in southern African during SAFARI 2000. *Remote Sensing of Environment*, 92, 255 - 275.

Miura, T., Huete, A. R., van Leeuwen, W. J. .D, and Didan, K., 1998, Vegetation detection through smoke filled AVIRIS images: An assessment using MODIS band passes. *Journal of Geophysical Research*, 103 (D24), 32001-32011.

Mouillot, F., Schultz, M. G., Yue, C., Cadule, P., Tansey, K., Ciais, P., and Chuvieco, E., 2013, Ten years of global burned area products from spaceborne remote sensing – A review: Analysis of user needs and recommendations for future developments. *International Journal of Applied Earth Observation and Geoinformation*, 26, 64-79.

Murphy, R. E., Ardanuy, P. Deluccia, F. J., Clement, C. E., and Schueler, C. E., 2006, The Visible Infrared Imaging Radiometer Suite. In *Earth Science Satellite Remote Sensing, Volume 1: Science and Instruments*, edited by J. J. Qu, W. Gao, M. Kafatos, R. E. Murphy, and V. V. Salomonson. Tsinghua University Press and Springer-Verlag, p. 199-223.

Pausas, J. G., and Fernández-Muñoz, S., 2012, Fire regime changes in the Western Mediterranean Basin: from fuel-limited to drought-driven fire regime. *Climatic change*, 110 (1-2), 215-226.

Roy, D.P., Boschetti, L., Justice, C.O., and Ju, J., 2008, The collection 5 MODIS burned area product - Global evaluation by comparison with the MODIS active fire product. *Remote Sensing of Environment*, 112, 3690-3707.

Roy, D. P., Frost, P. G .H., Justice, C. O., Landmann, T., Le Roux, J. L., Gumbo, K., Makungwa, S., Dunham, K., Du Toit, R., Mhwandagara, K., Zacarias, A., Tacheba, B., Dube, O. P., Pereira, J. M. C., Mushove, P., Morisette, J. T., Vannan, S. K. S., and Davies, D., 2005a, The Southern Africa Fire Network (SAFNet) regional burned-area product validation protocol. *International Journal of Remote Sensing*, 26, 4265-4292.

Roy, D. P., Jin, Y., Lewis, P. E., and Justice, C. O., 2005b, Prototyping a global algorithm for systematic fire-affected area mapping using MODIS time series data. *Remote Sensing of Environment*, 97, 137-162.

Roy, D.P., Lewis, P., Justice, C., 2002, Burned area mapping using multi-temporal moderate spatial resolution data - a bi-directional reflectance model-based expectation approach, *Remote Sensing of Environment*, 83:263-286.

Sukhinin, A. I., French, N. H. F., Kasischke, E. S., Hewson, J. H., Soja, A. J., Csiszar, I. A., Hyer, E. J., Loboda, T., Conard, S. G., Romasko, V. I., Pavlichenko, E. A., Miskiv, S. I., and Slinkina, O. A., 2004, Satellite-based mapping of fires in Russia: New products for fire management and carbon cycle studies. *Remote Sensing of Environment*, 93, 546–564.

Swap, R. J., Annegarn, H. J., Suttles, J. T., Haywood, J., Helmlinger, M. C., Hely, C., Hobbs, P. V., Holben, B. N., Ji, J., King, M., Landmann, T., Maenhaut, W., Otter, L., Pak, B., Piketh, S. J., Platnick, S., Privette, J., Roy, D. P., Thompson, A. M., Ward, D., Yokelson, R., 2002, The Southern African Regional Science Initiative (SAFARI 2000): overview of the dry-season field campaign. *South African Journal of Science*, 98, 125-130.

Trigg, S., and Flasse, S., 2000, Characterizing the spectral-temporal response of burned savannah using in situ spectroradiometry and infrared thermometry. *International Journal of Remote Sensing*, 21, 3161-3168.

van der Werf, G. R., Randerson, J. T., Giglio, L., Collatz, G. J., Mu, M., Kasibhatla, P. S., Morton, D. C., DeFries, R. S., Jin, Y., and van Leeuwen, T. T., 2010, Global fire emissions and the contribution of deforestation, savanna, forest, agricultural, and peat fires (1997-2009). *Atmospheric Chemistry and Physics*, 10, 11707-11735.

Westerling, A. L., Hidalgo, H. G., Cayan, D. R., and Swetnam, T. W., 2006, Warming and earlier spring increase western US forest wildfire activity. *Science*, 313, 940 – 943

Zarco-Tejada, P. J., Rueda, C. A., and Ustin, S. L., 2003, Water content estimation in vegetation with MODIS reflectance data and model inversion methods. *Remote Sensing of Environment*, 85, 109-124.

Acknowledgment

Material from the MODIS Fire Product ATBD has been included in this document.